Title:
Inhibition and stimulation of the human breast cancer resistance protein as in vitro predictor of drug-drug interactions of drugs of abuse.

Authors:
Lea Wagmann, Hans H. Maurer, Markus R. Meyer

This is a post-peer-review, pre-copyedit version of an article published in *Archives of Toxicology* (Volume 92, Pages 2875–2884, DOI: 10.1007/s00204-018-2276-y).
The final authenticated version is available online at: https://doi.org/10.1007/s00204-018-2276-y

Inhibition and stimulation of the human breast cancer resistance protein as in vitro predictor of drug-drug interactions of drugs of abuse

Lea Wagmann, Hans H. Maurer, and Markus R. Meyer

✉ Markus R. Meyer
markus.meyer@uks.eu

Department of Experimental and Clinical Toxicology, Institute of Experimental and Clinical Pharmacology and Toxicology, Center for Molecular Signaling (PZMS), Saarland University, 66421 Homburg, Germany

Abstract

Transporter-mediated drug-drug interactions (DDI) may induce adverse clinical events. As drugs of abuse (DOA) are marketed without preclinical safety studies, only very limited information about interplay with membrane transporters are available. Therefore, 13 DOA of various classes were tested for their in vitro affinity to the human breast cancer resistance protein (hBCRP), an important efflux transporter. As adenosine 5'-triphosphate (ATP) hydrolysis is crucial for hBCRP activity, adenosine 5'-diphosphate (ADP) formation was measured and used as in vitro marker for hBCRP ATPase activity. ADP quantification was performed by hydrophilic interaction liquid chromatography coupled to high resolution tandem mass spectrometry and its amount in test compound incubations was compared to that in reference incubations using the hBCRP substrate sulfasalazine or the hBCRP inhibitor orthovanadate. If DOA caused stimulation or inhibition, further investigations such as Michaelis-Menten kinetic modeling or IC_{50} value determination were conducted. Among the tested DOA, seven compounds showed statistically significant hBCRP ATPase stimulation. The entactogen 3,4-BDB and the plant alkaloid mitragynine were identified as strongest stimulators. Their affinity to the hBCRP ATPase was lower than that of sulfasalazine but comparable to that of rosuvastatin, another hBCRP model substrate. Five DOA showed statistically significant hBCRP ATPase inhibition. Determination of IC_{50} values identified the synthetic cannabinoid receptor agonists JWH-200 and WIN 55,212-2 as strongest inhibitors comparable to orthovanadate. The present study clearly demonstrated that tested DOA show in part high affinities to the hBCRP within the range of model substrates or inhibitors. Thus, there is a risk of hBCRP-mediated DDI, which needs to be considered in clinical settings.

Keywords Drugs of abuse, hBCRP, drug-drug interactions, mass spectrometry, HILIC

Introduction

Efflux transporters such as the human breast cancer resistance protein (hBCRP) can significantly influence absorption, distribution, and excretion of drugs. In analogy to its close relative P-glycoprotein (P-gp), the hBCRP is primarily present in sites critical for drug disposition, such as epithelia of the intestine or liver and the endothelium of the blood-brain barrier (International Transporter et al. 2010). Consequently, it decisively codetermines not only bioavailability and thus therapeutic efficacy but also drug-drug interactions (DDI), which can increase toxicity and encourage adverse drug reactions.

Interactions occur if translocation of a drug is influenced by a second compound either via inhibition or induction of the transport protein (Muller and Fromm 2011). Significantly increased plasma concentrations of hBCRP substrates after oral co-administration of an hBCRP inhibitor are described (Kruijtzer et al. 2002; Wang et al. 2018) and clinically relevant effects are expected in case of narrow therapeutic windows and toxic properties. However, it is important to note that transporter-based interactions may result in concentration changes of the substrate in a particular tissue without affecting the plasma concentration of the substrate followed by local toxic effects (Endres et al. 2006). This demonstrates the complexity of identifying toxicity mechanisms in vivo and underlines the importance of investigations of drug-transporter interactions in early stages of drug development.

As the impact of transporters on clinically relevant DDI is now generally recognized to be equal to that of drug metabolizing enzymes (Mao et al. 2018), new drug candidates are recommended to be routinely checked for interactions with the hBCRP and further transport proteins (International Transporter et al. 2010). Guidelines on the investigation of drug interactions were for example published by the European Medicines Agency (EMA) or the Food and Drug Administration (EMA 2012; FDA 2017). Unfortunately, only scarce information is available for interplay between the hBCRP and drugs of abuse (DOA), which are marketed without preclinical safety studies. hBCRP inhibition was only described for the abused alkaloid ibogaine and the plant cannabinoids cannabinol, cannabidiol, and delta 9-tetrahydrocannabinol (Holland et al. 2007; Tournier et al. 2010) demonstrating that DOA have to be considered. However, nothing is known about interactions with the so-called new psychoactive substances and profound toxicological risk assessment is ruled out. Sold as in part legal alternatives to drugs under international control with similar structures and effects, these compounds pose an outstanding risk as they proliferate at an unprecedented rate reaching almost 500 different substances in 2015 (UNODC 2017).

Therefore, the aim of the present study was to test 13 DOA with various chemical structures (Fig. 1) for their influence on the hBCRP. Primarily, in vitro experiments are recommended to identify potential factors influencing drug disposition, to elucidate potential DDI mechanisms, and to yield kinetic parameters for use in further studies (FDA 2017). Cell-based assays or membrane-based systems are suitable to get a first indication of hBCRP involvement. The latter is usually based on measurement of substrate-dependent adenosine 5'-triphosphate (ATP) hydrolysis, as the presence of ATP is crucial for an hBCRP-mediated transport. Thanks to this linking between substrate transport and catalytic activity followed by release of adenosine 5'-diphosphate (ADP) and inorganic phosphate, the ATPase activity can be used as in vitro marker for hBCRP transport (Sarkadi et al. 2006). Because of its simplicity and reproducibility, the ATPase assay is one of the most widely used in vitro models for identification of compounds that interact with the hBCRP (Sarkadi et al. 2006).

Recently, a validated ADP quantification method based on hydrophilic interaction liquid chromatography coupled to high resolution tandem mass spectrometry (HILIC-HRMS/MS) was published and successfully applied for determination of the in vitro hBCRP ATPase activity in presence of five HIV protease inhibitors (Wagmann et al. 2017b). This method in combination with the presented initial hBCRP ATPase activity screening procedure (Fig. 2) was applied in the current study for DOA testing at three different concentrations (5, 50, 500 µM) to get a first impression of their ATPase stimulation or inhibition potential. Further data was generated and used to calculate Michaelis-Menten kinetic parameters or IC_{50} values in case of stimulation or inhibition, respectively. We also investigated a model inhibitor (orthovanadate) and two model substrates (sulfasalazine and rosuvastatin) to clearly demonstrate suitable experimental conditions and to compare their data with those elucidated for the DOA.

Materials and methods

Chemicals and enzymes

Baculovirus-infected insect cell microsomes (Supersomes) containing complementary DNA-expressed hBCRP (Arg482, 5 mg protein/mL) and wild-type Supersomes without hBCRP (control membrane, 5 mg protein/mL) used as negative control were obtained from Corning (Amsterdam, The Netherlands). After delivery, Supersomes were thawed at 37 °C, aliquoted, snap-frozen in liquid nitrogen, and stored at -80 °C until use. ADP sodium salt, ATP magnesium salt, sulfasalazine, rosuvastatin, sodium orthovanadate, ammonium acetate, MES hydrate, and TRIS base were obtained from Sigma-Aldrich (Taufkirchen, Germany), formic acid (MS grade) from Fluka (Neu-Ulm, Germany), acetonitrile, methanol (both LC-MS grade), and all other chemicals from VWR (Darmstadt, Germany).

The test compounds *R,S*-1-(3,4-methylenedioxyphenyl)-2-butamine (3,4-BDB) and 1-[2-(4-morpholinyl)ethyl]-1H-indol-3-yl-(1-naphthyl)methanone (JWH-200) were supplied by Lipomed AG (Arlesheim, Switzerland), *R,S*-2-(benzylamino)-1-(4-methylphenyl)-1-propanone (benzedrone), diclofensine, *R,S*-1-(1,3-benzodioxol-5-yl)-2-(benzylamino)-1-propanone (3,4-MDBC), and *R,S*-1-(2-naphthyl)-2-(1-pyrrolidinyl)-1-pentanone (naphyrone) by LG Chemicals (Teddington, UK), *R,S*-1-(1,3-benzodioxol-5-yl)-2-(methylamino)-1-butanone (butylone) HCl by www.EU-Legals.com (currently not available) before it was scheduled, *R,S*-1-(4-iodo-2,5-dimethoxyphenyl)-2-propanamine (DOI) by Sigma-Aldrich, and [(3*R*)-5-methyl-3-(4-morpholinylmethyl)-2,3-dihydro[1,4]oxazino[2,3,4-hi]indol-6-yl](1-naphthyl)methanone (WIN 55,212) mesylate by Chiron AS (Trondheim, Norway). (6a*S*)-1,2,9,10-tetramethoxy-6-methyl-5,6,6a,7-tetrahydro-4H-dibenzo[de,g]quinoline (glaucine) HBr was obtained from Oskar Tropitzsch (Marktredwitz, Germany), *N*-(1-phenylcyclohexyl)-3-ethoxypropanamine (PCEPA) HCl was provided by the Hessisches Landeskriminalamt (Wiesbaden, Germany), and methyl(E)-2-[(2*S*,3*S*,12b*S*)-3-ethyl-8-methoxy-1,2,3,4,6,7,12,12b-octahydroindolo[2,3-a]quinolizin-2-yl]-3-methoxyprop-2-enoate (mitragynine) by the Department of Forensic Medicine, Johannes Gutenberg University (Mainz, Germany), where it was isolated from kratom leaves obtained from head&nature (Regensburg, Germany) (Philipp et al. 2009). *N*-Allyl-*N*-[2-(5-methoxy-1H-indol-3-yl)ethyl]-2-propen-1-amine (5-MeO-DALT) was synthesized by use of established methods (Brandt et al. 2008) and provided by the School of Pharmacy and Biomolecular Sciences, John Moores University (Liverpool, UK).

Preparation of stock solutions

Stock solutions were prepared in bidistilled water for sodium orthovanadate (10 mM), ADP, and ATP (20 mM, respectively) or in methanol for sulfasalazine (0.5 mg/mL), rosuvastatin, and the test compounds (1 mg/mL, respectively). Stock solutions were aliquoted and stored at -20 °C until use. To ensure that the organic solvent content in the final incubation mixtures was not higher than 3% (Chauret et al. 1998), methanolic stock solutions were gently evaporated under nitrogen at 70 °C and resolved in water/methanol (8:2, v/v) in a final concentration of 15 mM prior to incubations. To exclude negative impacts on the analytes' concentration, their peak areas in a concentration of 0.5 mM diluted with acetonitrile from the methanolic stock solutions or the resolved solutions were compared. The MS settings were the same as described before (Helfer et al. 2015). A peak area decrease of 30% was defined as tolerable and this criterion was fulfilled for all test compound solutions.

HILIC-HRMS/MS apparatus

A Thermo Fisher Scientific (TF, Dreieich, Germany) Dionex UltiMate 3000 Rapid Separation (RS) UHPLC system with a quaternary UltiMate 3000 RS pump and an UltiMate 3000 RS autosampler was used and controlled by the TF Chromeleon software version 6.80. It was coupled to a TF Q-Exactive Plus mass spectrometer equipped with a heated electrospray ionization II source (HESI-II). Conditions and settings were the same as described previously (Wagmann et al. 2017b). Briefly, gradient elution was performed on a Macherey-Nagel (Düren, Germany) HILIC Nucleodur column (125 × 3 mm, 3 µm) using aqueous ammonium acetate (200 mM, eluent A) and acetonitrile containing 0.1% (*v/v*) formic acid (eluent B). The flow rate was set to 700 µL/min and an isocratic elution with a duration of 6 min using 65% eluent B was performed at 40 °C column temperature, maintained by a Dionex UltiMate 3000 RS analytical column heater. The injection volume for all samples was 1 µL. HESI-II conditions were: sheath gas, 60 arbitrary units (AU); auxiliary gas, 10 AU; spray voltage, 4.00 kV; heater temperature, 320 °C; ion transfer capillary temperature, 320 °C; and S-lens RF level, 60.0. Mass calibration was done prior to analysis according to the manufacturer's recommendations using external mass calibration. ADP quantification was performed using a targeted single ion monitoring (t-SIM) and a subsequent data-dependent MS^2 (dd-MS^2) mode with an inclusion list containing the exact masses of negatively charged adenosine 5'-monophosphate (AMP, *m/z* 346.0558), ADP (*m/z* 426.0221), and ATP (*m/z* 505.9885). The settings for the t-SIM mode were as follows: microscan, 1; resolution, 35,000; AGC target, 5e4; maximum IT, 100 ms; and isolation window, 4 *m/z*. The settings for the dd-MS^2 mode were as follows: microscan, 1; resolution, 35,000; AGC target, 2e5; maximum IT, 100 ms; isolation window, 4 *m/z*; and dynamic exclusion, 4 s. TF Xcalibur Qual Browser 2.2 software was used for data handling. The settings for automated peak integration were as follows: mass tolerance, 5 ppm; peak detection algorithm, ICIS; area noise factor, 5; and peak noise factor, 300. GraphPad QuickCalcs (GraphPad Software, San Diego, USA) was used for outlier detection (http://graphpad.com/quickcalcs/grubbs1), while GraphPad Prism 5.00 software was used for statistical evaluation.

Before analysis of study samples, two blank samples, six levels of calibration standards in duplicate, and three levels of quality control (QC) samples in duplicate were measured. ADP concentrations of calibrators and QC samples are given in Table 1. Blank samples only contained control membranes (0.2 mg/mL) and ATP (4 mM), while calibrators and QC samples contained the particular ADP amount as well. Prior to analysis, they were diluted with acetonitrile (1:1, *v/v*). These samples as well as the study samples were analyzed twice and the mean ADP area minus mean ADP area in blank samples or blank incubations was used for quantification (Wagmann et al. 2017b).

Initial hBCRP ATPase activity screening

To check whether the test compounds had an influence on the hBCRP ATPase activity, four different sample sets consisting of three samples each were used. A simplified scheme of the hBCRP ATPase activity screening procedure is given in Fig. 2. Setup and incubation conditions were the same as previously described with minor modifications (Wagmann et al. 2017b). Briefly, sample set one contained hBCRP membrane, ATP, and one of the test compounds, while sample set two additionally contained sulfasalazine. Sample set three consisted of hBCRP membrane, ATP, and sulfasalazine, while sample set four contained orthovanadate in addition. All reactions were started by addition of ATP and stopped after 10 min of incubation at 37 °C by addition of 30 µL of ice-cold acetonitrile. The mixture was centrifuged for 2 min at 10,000×*g*, the supernatant transferred to an autosampler vial, and analyzed by HILIC-HRMS/MS. Prior to incubations, hBCRP membrane was diluted with TRIS-MES buffer (pH 6.8), while ATP, sulfasalazine, orthovanadate, and the test compounds were diluted with bidistilled water. Final concentrations were 0.2 mg/mL hBCRP, 4 mM ATP, 10 µM sulfasalazine, and 400 µM orthovanadate. Three different concentration levels of the test compounds were used (5, 50, and 500 µM). Furthermore, a blank set consisting of three samples only containing ATP and control membranes (0.2 mg/mL) were incubated and measured. ADP in these blank incubations was subtracted from ADP in all other sample sets. In addition, an interference set consisting of three samples containing hBCRP membrane, ATP, and sulfasalazine were incubated and the reactions were stopped with acetonitrile containing one of the test compounds in a concentration of 500 µM instead of pure acetonitrile.

Finally, ADP was quantified and its formation in set three was always set to 100% and ADP formation in all the sample sets was compared to each other. To detect ATPase stimulation, set one was compared to set four, while set two was compared to set three to detect ATPase inhibition (Fig. 2). ADP formation in the interference set should be equal to that in set three. To decide whether detected ADP formation differences were statistically significant or not, a one-way ANOVA was performed followed by Dunnett's multiple comparison test (***, $P < 0.001$, **, $P < 0.01$, *, $P < 0.05$) using GraphPad Prism 5.00 software. Further investigations of kinetic constants and/or IC_{50} values of the test compounds were only conducted if a significant difference of at least $P < 0.01$ was detected for a minimum of one concentration level.

Kinetic studies

The kinetic constants were derived from incubations with hBCRP membranes. Substrate concentrations were chosen to allow modeling of enzyme kinetics and were always between 0.005 and 500 µM. ATP (4 mM) was additionally contained in the final incubation mixtures. Incubation time and hBCRP membrane concentration were chosen to be in the linear range of ADP formation and final conditions given in Table 2. Blank incubations only contained hBCRP membrane and ATP and the ADP amount found in these incubations was subtracted from ADP in the other incubations. All incubations were performed in triplicate. Kinetic constants were calculated by ADP quantification using a calibration curve (Table 1). Enzyme kinetic constants were estimated by nonlinear curve fitting using GraphPad Prism 5.00 software. The Michaelis-Menten equation (Eq. (1)) was used to calculate apparent K_m and V_{max} values, where v is the initial reaction velocity, S the substrate concentration, V_{max} the maximal reaction velocity, and K_m the substrate concentration at half V_{max}.

$$v = \frac{V_{max} \times S}{K_m + S} \quad (1)$$

Determination of IC_{50} values

Inhibitors were incubated at ten different concentrations (5, 10, 20, 39, 78, 156, 313, 625, 1250, 2500 µM), with exception of JWH-200 and WIN 55,212-2, which could not be incubated at 2500 µM due to insufficient solubility. Sulfasalazine (10 µM), ATP (4 mM), and hBCRP membrane (0.2 mg/mL) were additionally contained in the final incubation mixtures. Control incubations without inhibitor and blank incubations were also prepared. Blank incubations only contained control membranes and ATP. The ADP amount found in these incubations was subtracted from ADP in the other incubations. All incubation conditions were the same as described for the initial hBCRP ATPase activity screening. All incubations were conducted in duplicate. The IC_{50} values were calculated by plotting the metabolite formation (relative to the control incubations) over the logarithm of the inhibitor concentration using GraphPad Prism 5.00.

Results

Initial hBCRP ATPase activity screening

ADP was quantified and its formation in the different sample sets (Fig. 2) was compared. ADP formation in sample set three (set to 100% hBCRP ATPase activity) and the interference set were found to be not significantly different. Residual hBCRP ATPase activity in sample set four containing sulfasalazine and orthovanadate ranged always between 1 and 8%.

Results for detection of hBCRP ATPase stimulators are given in Table 3. In total, rosuvastatin and seven DOA demonstrated hBCRP ATPase stimulation potential. In comparison to these incubations, rosuvastatin showed statistically significant higher ADP formation in all tested concentrations. The DOA butylone, DOI, JWH-200, and mitragynine also activated the hBCRP ATPase in all tested concentration levels, whilst 3,4-BDB only showed an effect in the highest concentration, WIN 55,212-2 in the lowest concentration, and diclofensine at the lowest and the medium concentration. However, detected stimulation by rosuvastatin or DOA was lower than that detected in sample set three caused by 10 µM sulfasalazine.

Results for detection of hBCRP ATPase inhibitors are given in Table 4. In total, five DOA provided an hBCRP ATPase inhibition potential. In comparison to incubations with sulfasalazine alone, all of these compounds showed statistically significant reduction of ADP formation at their highest concentration level. Only JWH-200 and WIN 55,212-2 also showed an effect at medium concentration.

Kinetic studies

The enzyme kinetic curves of sulfasalazine and rosuvastatin are depicted in Fig. 3. Kinetic curves of 3,4-BDB and mitragynine are given in Fig. 4. K_m and V_{max} values are summarized in Table 5.

Determination of IC_{50} values

IC_{50} values of orthovanadate and the five DOA are given in Table 6. The determined IC_{50} values were between 13 and 359 µM. Amongst the DOA, the synthetic cannabinoid receptor agonists JWH-200 and WIN 55,212-2 provided the lowest IC_{50} values, comparable to that of orthovanadate.

Discussion

As already mentioned, hBCRP ATPase activity is a widely-used in vitro model to get a first impression of interactions between test compounds and efflux transporters. As ATP hydrolysis is substrate-dependent, ATPase activity increases in the presence of transported substrates, while noncompetitive inhibitors reduce the ATPase activity of the investigated transport protein (Sarkadi et al. 2006). If ATP is hydrolyzed, inorganic phosphate and ADP are released. The latter can be quantified and used as in vitro marker for hBCRP ATPase activity (Wagmann et al. 2017b). Direct analysis of the product ADP, by use of HILIC-HRMS/MS, is less interference-prone than colorimetric measurement of inorganic phosphate or bioluminescence-based analysis of residual ATP (Kaskova et al. 2016; Upreti 1984). However, drawbacks of the ATPase assay include inconsistency between ATPase activity and the transport rate of some substrates and inhibitors, a high incidence of false positives and negatives, and the requirement of high substrate concentrations (International Transporter et al. 2010). Nevertheless, notable advantages are simplicity, reproducibility, and particularly cost-effectiveness, as hBCRP expressing membrane fragments can be used, which are cheaper than membrane vesicles or cell culture experiments.

To extend the knowledge surrounding interactions between DOA and the hBCRP, 13 DOA were tested for their influence on the hBCRP ATPase. These test compounds belonged to various DOA classes for example stimulants, entactogens, or synthetic cannabinoid receptor agonists and provided different chemical structures (Fig. 1). All of them were shown previously to be stimulators of the P-gp ATPase and/or P-gp inhibitors using polarized cell monolayers (Meyer et al. 2013; Meyer et al. 2015). As a broad overlap between P-gp and hBCRP substrates was described (Hira and Terada 2018), these compounds were now investigated for their influence on the hBCRP ATPase.

The used initial hBCRP ATPase activity screening setup was already successfully applied for investigation of five HIV protease inhibitors. Amongst them, three were identified as hBCRP inhibitors (Wagmann et al. 2017b). However, none of them showed hBCRP ATPase stimulation and therefore the known stimulator rosuvastatin (Huang et al. 2006) was used as control. As only adenosine phosphates were analytically detected, it was mandatory to investigate the influence of all test compounds on the ADP MS signal. Both, enhancement or suppression of the ADP signal could lead to errors in assessing a compound's hBCRP substrate or inhibitor properties. However, no analytical interferences were detected as the ADP formation in the interference set and sample set three were always similar. Furthermore, sample set four provided minimal residual hBCRP ATPase activity what confirmed almost complete hBCRP inhibition by orthovanadate.

The EMA defined that in case of DDI, one compound acts as victim drug and the other one as perpetrator drug. The victim drug is the compound affected by DDI, while the perpetrator drug is that one, which affects the pharmacokinetic and/or pharmacodynamic properties of the victim drug (EMA 2012). In the context of hBCRP-mediated interactions, an hBCRP substrate would rather act as victim, while an inhibitor would be the perpetrator. Both possibilities should be considered and investigated and therefore hBCRP ATPase stimulators as well as inhibitors should be identified.

According to the previous study, ADP formation in sample set one was initially compared to that in sample set three to detect hBCRP ATPase stimulators (Wagmann et al. 2017b). ADP formation in rosuvastatin incubations was found to be significantly lower than ADP formation in sample set three, indicating that rosuvastatin was either no or a weaker hBCRP substrate than sulfasalazine. However, sulfasalazine is widely accepted as ideal hBCRP probe substrate (Jani et al. 2009), causing intense hBCRP ATPase stimulation, which is probably stronger than that caused by other hBCRP substrates. Therefore, ADP formation in sample set one

was compared to that in sample set four instead of sample set three to identify also weaker hBCRP ATPase stimulators than sulfasalazine. This alignment had no influence on the negative assessment of the hBCRP ATPase stimulation properties of the HIV protease inhibitors, which were previously reported to be no hBCRP substrates (Gupta et al. 2004). Even if rosuvastatin and seven DOA were shown to have hBCRP ATPase stimulation properties, maximum ATPase activity was always less than 50% of that caused by sulfasalazine. As already mentioned above, the hBCRP ATPase stimulation caused by sulfasalazine was expected to be more pronounced than that generated by other hBCRP substrates. The findings are in line with this assumption. As highest hBCRP ATPase activities were mainly caused by the medium test compound concentration (50 µM), the occurrence of substrate-dependent inhibition at higher concentrations is likely.

To identify potential hBCRP ATPase inhibitors, ADP formation in sample set two was compared to that in sample set three. Five DOA were shown to have hBCRP ATPase inhibition potential. To reduce the hBCRP ATPase activity rather high concentrations of 3,4-BDB, diclofensine, or mitragynine were needed, compared to lower concentrations of JWH-200 or WIN 55,212-2. It is notable, that all of these inhibitory substances also showed stimulating properties in the initial hBCRP ATPase activity screening, what could indicate a partial competitive inhibition mechanism. However, in case of rosuvastatin, no inhibitory properties were detected in co-incubations with sulfasalazine.

The initial hBCRP ATPase activity screening demonstrated that only selected DOA had an influence on the hBCRP ATPase activity. As only these substances were further investigated by kinetic studies or IC_{50} value determination, time and costs could be saved. Such prescreening procedures were already successfully applied to detect interactions with other enzymes (Dinger et al. 2016; Wagmann et al. 2017a).

The Michaelis-Menten kinetics of sulfasalazine and rosuvastatin (Fig. 3) were modeled as controls to demonstrate that the chosen incubation conditions were suitable. Determined K_m values were similar to published K_m values for sulfasalazine (0.70 µM) (Jani et al. 2009) or rosuvastatin (10.8 µM) (Huang et al. 2006), respectively. Not only the K_m value of sulfasalazine was lower than that of rosuvastatin but also its V_{max} value was higher. Both parameters indicated that sulfasalazine is a stronger hBCRP substrate than rosuvastatin, as already assumed after the initial hBCRP ATPase activity screening. Concerning DOA, 3,4-BDB provided a K_m value comparable to that of rosuvastatin, while the K_m value of mitragynine was higher. Determined V_{max} values of the test compounds were lower than V_{max} values of the model substrates indicating a slower transport rate of the DOA. Although butylone, diclofensine, DOI, JWH-200, and WIN 55,212-2 showed initial activity in the screening studies, enzyme kinetics could finally not be modeled due to insufficient activities.

For presumed hBCRP ATPase inhibitors, the inhibitor concentration at which the enzyme activity is reduced by 50% should be determined. This concentration is expressed as IC_{50} value. To demonstrate that chosen incubation conditions were suitable, the IC_{50} value of the model inhibitor orthovanadate was determined and comparable to that described in literature (20 µM) (Ishikawa et al. 2003). Additionally, IC_{50} values of five DOA were determined. To predict a potential clinical relevance of the hBCRP inhibition based on IC_{50} values, expected plasma concentrations (given in Table 6) should be considered. Unfortunately, only limited information concerning DOA plasma concentrations is available. Generally, case reports are the only information source and interpretation is difficult due to single cases, polytoxicomania, or post mortem concentrations that are affected by post mortem redistribution (Staeheli et al. 2017). In case of 3,4-BDB only a single post mortem concentration was published and in this case 2.1 mg/L amphetamine and 0.4 mg/L *N*-methyl-1-(3,4-methylenedioxyphenyl)-2-butamine (3,4-MBDB) were additionally detected (Carter et al. 2000). Diclofensine is abused due to central

stimulating properties but was originally developed as antidepressant (Meyer et al. 2015). Published concentrations were derived from a controlled experiment after intake of doses common for antidepressant therapy (Strojny and de Silva 1985) and are therefore not necessarily equal to doses in case of abuse. Mitragynine concentrations were determined in 10 chronic kratom users with the aim of investigating its pharmacokinetics (Trakulsrichai et al. 2015). As plasma concentrations after intake of JWH-200 or WIN 55,212-2 have not yet been determined, those published for over 20 other synthetic cannabinoid receptor agonists such as JWH-018, JWH-122, or JWH-203 were used. The given concentrations derived from a trail to investigate JWH-018 pharmacokinetics, driving under the influence of drug cases, intoxications, or autopsies (Karinen et al. 2015; Toennes et al. 2017). This fact and the large number of different synthetic cannabinoid receptor agonists explained the broad concentration ranges. In summary, expected DOA plasma concentrations were lower than the determined IC_{50} values. Therefore, a clinical effect seemed rather unlikely. However, it must be considered that concentrations in certain tissues are often higher than in plasma. This is for example more than likely in the liver, the main metabolizing organ. Thus, the occurrence of local DDI (Endres et al. 2006) followed by local toxicity cannot be excluded, especially not after intake of high doses.

Conclusions

The present study was the first to describe the influence of a broad range of new DOA on the hBCRP ATPase activity. A recently published ADP quantification method and the initial hBCRP ATPase activity screening procedure were successfully applied for DOA testing. The results demonstrated that DOA can act as hBCRP ATPase stimulators or inhibitors. 3,4-BDB and mitragynine were shown to have an hBCRP ATPase stimulation potential. Thanks to the determination of kinetic parameters, their transport is expected to be slower than that of the model substrates. Nevertheless, they could act as victim drug in case of co-consumption of an hBCRP inhibitor followed by potential (local) toxic effects. JWH-200 and WIN 55,212-2 were identified as hBCRP inhibitors comparably strong as the model inhibitor. Therefore, they could act as perpetrator drug, especially after intake of high doses. However, as in vitro studies only have a limited conclusiveness, further investigations are warranted to facilitate a more complete assessment.

Acknowledgements The authors like to thank Achim T. Caspar, Lilian H. J. Richter, Gabriele Ulrich, and Armin A. Weber for their support.

Conflict of interest The authors declare that they have no conflict of interest.

Table 1 ADP concentrations of calibrators and quality control (QC) samples.

	Calibrator						QC sample		
	1	2	3	4	5	6	low	medium	high
ADP conc., µM	50	100	200	300	400	500	125	250	375

Table 2 Incubation time and hBCRP membrane concentration for determination of kinetic constants.

Test compound	Incubation time, min	hBCRP conc., mg/mL
3,4-BDB	30	0.4
Mitragynine	30	0.4
Sulfasalazine	10	0.2
Rosuvastatin	30	0.2

Table 3 Initial hBCRP ATPase activity screening results for detection of hBCRP ATPase stimulation. Percentage ADP formation (percentage error in brackets) represented ADP formation in incubations containing one of the test compounds in relation to incubations containing the hBCRP model substrate sulfasalazine (10 µM). Significant differences in comparison to reference incubations containing sulfasalazine and the hBCRP model inhibitor orthovanadate (400 µM) are marked by asterisks (***, $P < 0.001$, **, $P < 0.01$, *, $P < 0.05$).

	ADP formation, %								
Test compound	5 µM			50 µM			500 µM		
Rosuvastatin	30	(2)	***	41	(3)	***	34	(3)	***
3,4-BDB	19	(13)		13	(8)		32	(3)	***
Benzedrone	23	(3)	*	16	(1)		15	(7)	
Butylone	27	(2)	**	29	(3)	**	34	(2)	***
Diclofensine	31	(4)	***	26	(3)	**	11	(2)	
DOI	29	(7)	**	30	(6)	***	26	(2)	**
Glaucine	13	(5)		16	(7)		16	(7)	
JWH-200	16	(4)	***	29	(1)	***	17	(1)	***
3,4-MDBC	20	(2)		21	(3)	*	18	(4)	
5-MeO-DALT	13	(5)		16	(7)		16	(7)	
Mitragynine	27	(2)	***	39	(1)	***	25	(9)	**
Naphyrone	7	(2)		32	(9)	*	30	(1)	
PCEPA	18	(2)		15	(3)		21	(1)	*
WIN 55,212-2	12	(1)	**	6	(1)		4	(5)	

Table 4 Initial hBCRP ATPase activity screening results for detection of hBCRP ATPase inhibition. Percentage ADP formation (percentage error in brackets) represented ADP formation in incubations containing one of the test compounds in relation to incubations containing the hBCRP model substrate sulfasalazine (10 µM) and significant differences are marked by asterisks (***, P < 0.001, **, P < 0.01, *, P < 0.05).

	ADP formation, %								
Test compound	5 µM			50 µM			500 µM		
Rosuvastatin	126	(21)		129	(11)		84	(1)	
3,4-BDB	95	(8)		71	(13)		36	(16)	***
Benzedrone	96	(3)		92	(9)		73	(3)	*
Butylone	126	(3)	*	107	(14)		74	(1)	*
Diclofensine	93	(12)		97	(12)		20	(3)	***
DOI	110	(4)		105	(4)		88	(7)	
Glaucine	67	(9)		74	(21)		82	(3)	
JWH-200	78	(10)		30	(16)	***	22	(16)	***
3,4-MDBC	103	(1)		106	(17)		112	(25)	
5-MeO-DALT	81	(17)		86	(19)		84	(2)	
Mitragynine	86	(6)		72	(11)		31	(2)	***
Naphyrone	99	(9)		102	(7)		85	(5)	
PCEPA	74	(8)		102	(1)		77	(10)	
WIN 55,212-2	84	(4)		32	(3)	***	25	(2)	***

Table 5 K_m and V_{max} values of tested drugs of abuse, sulfasalazine, and rosuvastatin.

Test compound	K_m, µM			V_{max}, pmol/µg hBCRP/min		
3,4-BDB	2.3	±	1	5.7	±	0.5
Mitragynine	14	±	3	11	±	0.6
Sulfasalazine	0.68	±	0.1	128	±	6
Rosuvastatin	1.2	±	0.3	26	±	1

Table 6 Test compounds, reference plasma concentrations, and IC_{50} values (percentage error in brackets) for inhibition of hBCRP ATPase activity (PM: post mortem; DUID: driving under the influence of drug).

Test compound	Common plasma concentration µg/L	µM	IC_{50} value, µM
Drugs of abuse			
3,4-BDB	106 (PM) (Carter et al. 2000)	0.6	143 (1)
Diclofensine	5 (Strojny and de Silva 1985)	0.02	113 (1)
JWH-200	*0.1 - 28* # (DUID cases)	*0.0003 - 0.07* #	19 (8)
	0.1 - 320 # (intoxications)	*0.0003 - 0.8* #	
	0.1 - 199 # (PM) (Karinen et al. 2015)	*0.0003 - 0.5* #	
	3 - 10 # (Toennes et al. 2017)	*0.008 - 0.03* #	
Mitragynine	19 - 105 (Trakulsrichai et al. 2015)	0.05 - 0.3	359 (1)
WIN 55,212-2	*0.1 - 28* # (DUID cases)	*0.0002 - 0.07* #	15 (8)
	0.1 - 320 # (intoxications)	*0.0002 - 0.8* #	
	0.1 - 199 # (PM) (Karinen et al. 2015)	*0.0002 - 0.5* #	
	3 - 10 # (Toennes et al. 2017)	*0.007 - 0.02* #	
Known inhibitor			
Orthovanadate	-	-	13 (8)

no plasma concentrations published, listed concentrations were published for other synthetic cannabinoid receptor agonists

Legends to the figures

Fig. 1 Chemical structures of the investigated drugs of abuse.

Fig. 2 Simplified scheme of the initial hBCRP ATPase activity screening procedure.

Fig. 3 Kinetic curves modeled after incubation of different concentrations of sulfasalazine (left: 10 min incubation time, in presence of 4 mM ATP and 0.2 mg/mL hBCRP, n = 3) or rosuvastatin (right: 30 min incubation time, in presence of 4 mM ATP and 0.2 mg/mL hBCRP, n = 3).

Fig. 4 Kinetic curves modeled after incubation of different concentrations of 3,4-BDB (left: 30 min incubation time, in presence of 4 mM ATP and 0.4 mg/mL hBCRP, n = 3) or mitragynine (right: 30 min incubation time, in presence of 4 mM ATP and 0.4 mg/mL hBCRP, n = 3).

References

Brandt SD, Tirunarayanapuram SS, Freeman S, et al. (2008) Microwave-accelerated synthesis of psychoactive deuteratedN,N-dialkylated-[α,α,β,β-d4]-tryptamines. J Labelled Compd Radiopharm 51(14):423-429

Carter N, Rutty GN, Milroy CM, Forrest AR (2000) Deaths associated with MBDB misuse. Int J Legal Med 113(3):168-70

Chauret N, Gauthier A, Nicoll-Griffith DA (1998) Effect of common organic solvents on in vitro cytochrome P450-mediated metabolic activities in human liver microsomes. Drug Metab Dispos 26(1):1-4

Dinger J, Meyer MR, Maurer HH (2016) In vitro cytochrome P450 inhibition potential of methylenedioxy-derived designer drugs studied with a two-cocktail approach. Arch Toxicol 90(2):305-18

EMA (2012) Guideline on the investigation of drug interactions. vol CPMP/EWP/560/95/Rev. 1 Corr. 2** 2012 edn. European Medicines Agency, London, UK http://www.ema.europa.eu/docs/en_GB/document_library/Scientific_guideline/2012/07/WC500129606.pdf, 05-21-2018

Endres CJ, Hsiao P, Chung FS, Unadkat JD (2006) The role of transporters in drug interactions. Eur J Pharm Sci 27(5):501-17

FDA (2017) In Vitro Metabolism- and Transporter- Mediated Drug-Drug Interaction Studies, Guidance for Industry. FDA (Food and Drug Administration) https://www.fda.gov/downloads/Drugs/GuidanceComplianceRegulatoryInformation/Guidances/UCM581965.pdf, 05-21-2018

Gupta A, Zhang Y, Unadkat JD, Mao Q (2004) HIV protease inhibitors are inhibitors but not substrates of the human breast cancer resistance protein (BCRP/ABCG2). J Pharmacol Exp Ther 310(1):334-41

Helfer AG, Michely JA, Weber AA, Meyer MR, Maurer HH (2015) Orbitrap technology for comprehensive metabolite-based liquid chromatographic-high resolution-tandem mass spectrometric urine drug screening - exemplified for cardiovascular drugs. Anal Chim Acta 891:221-33

Hira D, Terada T (2018) BCRP/ABCG2 and high-alert medications: Biochemical, pharmacokinetic, pharmacogenetic, and clinical implications. Biochem Pharmacol 147:201-210

Holland ML, Lau DT, Allen JD, Arnold JC (2007) The multidrug transporter ABCG2 (BCRP) is inhibited by plant-derived cannabinoids. Br J Pharmacol 152(5):815-24

Huang L, Wang Y, Grimm S (2006) ATP-dependent transport of rosuvastatin in membrane vesicles expressing breast cancer resistance protein. Drug Metab Dispos 34(5):738-42

International Transporter C, Giacomini KM, Huang SM, et al. (2010) Membrane transporters in drug development. Nat Rev Drug Discov 9(3):215-36

Ishikawa T, Kasamatsu S, Hagiwara Y, Mitomo H, Kato R, Sumino Y (2003) Expression and functional characterization of human ABC transporter ABCG2 variants in insect cells. Drug Metab Pharmacokinet 18(3):194-202

Jani M, Szabo P, Kis E, Molnar E, Glavinas H, Krajcsi P (2009) Kinetic characterization of sulfasalazine transport by human ATP-binding cassette G2. Biol Pharm Bull 32(3):497-9

Karinen R, Tuv SS, Oiestad EL, Vindenes V (2015) Concentrations of APINACA, 5F-APINACA, UR-144 and its degradant product in blood samples from six impaired drivers compared to previous reported concentrations of other synthetic cannabinoids. Forensic Sci Int 246:98-103

Kaskova ZM, Tsarkova AS, Yampolsky IV (2016) 1001 lights: luciferins, luciferases, their mechanisms of action and applications in chemical analysis, biology and medicine. Chem Soc Rev 45(21):6048-6077

Kruijtzer CM, Beijnen JH, Rosing H, et al. (2002) Increased oral bioavailability of topotecan in combination with the breast cancer resistance protein and P-glycoprotein inhibitor GF120918. J Clin Oncol 20(13):2943-50

Mao Q, Lai Y, Wang J (2018) Drug Transporters in Xenobiotic Disposition and Pharmacokinetic Prediction. Drug Metab Dispos 46(5):561-566

Meyer MR, Orschiedt T, Maurer HH (2013) Michaelis-Menten kinetic analysis of drugs of abuse to estimate their affinity to human P-glycoprotein. Toxicol Lett 217(2):137-42

Meyer MR, Wagmann L, Schneider-Daum N, et al. (2015) P-glycoprotein interactions of novel psychoactive substances - stimulation of ATP consumption and transport across Caco-2 monolayers. Biochem Pharmacol 94(3):220-6

Muller F, Fromm MF (2011) Transporter-mediated drug-drug interactions. Pharmacogenomics 12(7):1017-37

Philipp AA, Wissenbach DK, Zoerntlein SW, Klein ON, Kanogsunthornrat J, Maurer HH (2009) Studies on the metabolism of mitragynine, the main alkaloid of the herbal drug Kratom, in rat and human urine using liquid chromatography-linear ion trap mass spectrometry. J Mass Spectrom 44(8):1249-61

Sarkadi B, Homolya L, Szakacs G, Varadi A (2006) Human multidrug resistance ABCB and ABCG transporters: participation in a chemoimmunity defense system. Physiol Rev 86(4):1179-236

Staeheli SN, Gascho D, Ebert LC, Kraemer T, Steuer AE (2017) Time-dependent postmortem redistribution of morphine and its metabolites in blood and alternative matrices-application of CT-guided biopsy sampling. Int J Legal Med 131(2):379-389

Strojny N, de Silva JA (1985) Determination of diclofensine, an antidepressant agent, and its major metabolites in human plasma by high-performance liquid chromatography with fluorometric detection. J Chromatogr 341(2):313-31

Toennes SW, Geraths A, Pogoda W, et al. (2017) Pharmacokinetic properties of the synthetic cannabinoid JWH-018 and of its metabolites in serum after inhalation. J Pharm Biomed Anal 140:215-222

Tournier N, Chevillard L, Megarbane B, Pirnay S, Scherrmann JM, Decleves X (2010) Interaction of drugs of abuse and maintenance treatments with human P-glycoprotein (ABCB1) and breast cancer resistance protein (ABCG2). Int J Neuropsychopharmacol 13(7):905-15

Trakulsrichai S, Sathirakul K, Auparakkitanon S, et al. (2015) Pharmacokinetics of mitragynine in man. Drug Des Devel Ther 9:2421-9

UNODC (2017) World Drug Report. United Nations publication https://www.unodc.org/wdr2017/index.html, 05-21-2018

Upreti GC (1984) Colorimetric estimation of inorganic phosphate in colored and/or turbid biological samples: assay of phosphohydrolases. Anal Biochem 137(2):485-92

Wagmann L, Brandt SD, Kavanagh PV, Maurer HH, Meyer MR (2017a) In vitro monoamine oxidase inhibition potential of alpha-methyltryptamine analog new psychoactive substances for assessing possible toxic risks. Toxicol Lett 272:84-93

Wagmann L, Maurer HH, Meyer MR (2017b) An easy and fast adenosine 5'-diphosphate quantification procedure based on hydrophilic interaction liquid chromatography-high resolution tandem mass spectrometry for determination of the in vitro adenosine 5'-triphosphatase activity of the human breast cancer resistance protein ABCG2. J Chromatogr A 1521:123-130

Wang X, Zhang ZY, Arora S, et al. (2018) Effects of Rolapitant Administered Intravenously or Orally on the Pharmacokinetics of Digoxin (P-glycoprotein Substrate) and Sulfasalazine (Breast Cancer Resistance Protein Substrate) in Healthy Volunteers. J Clin Pharmacol 58(2):202-211

Figure 1

Click here to download Figure Fig_1.tif

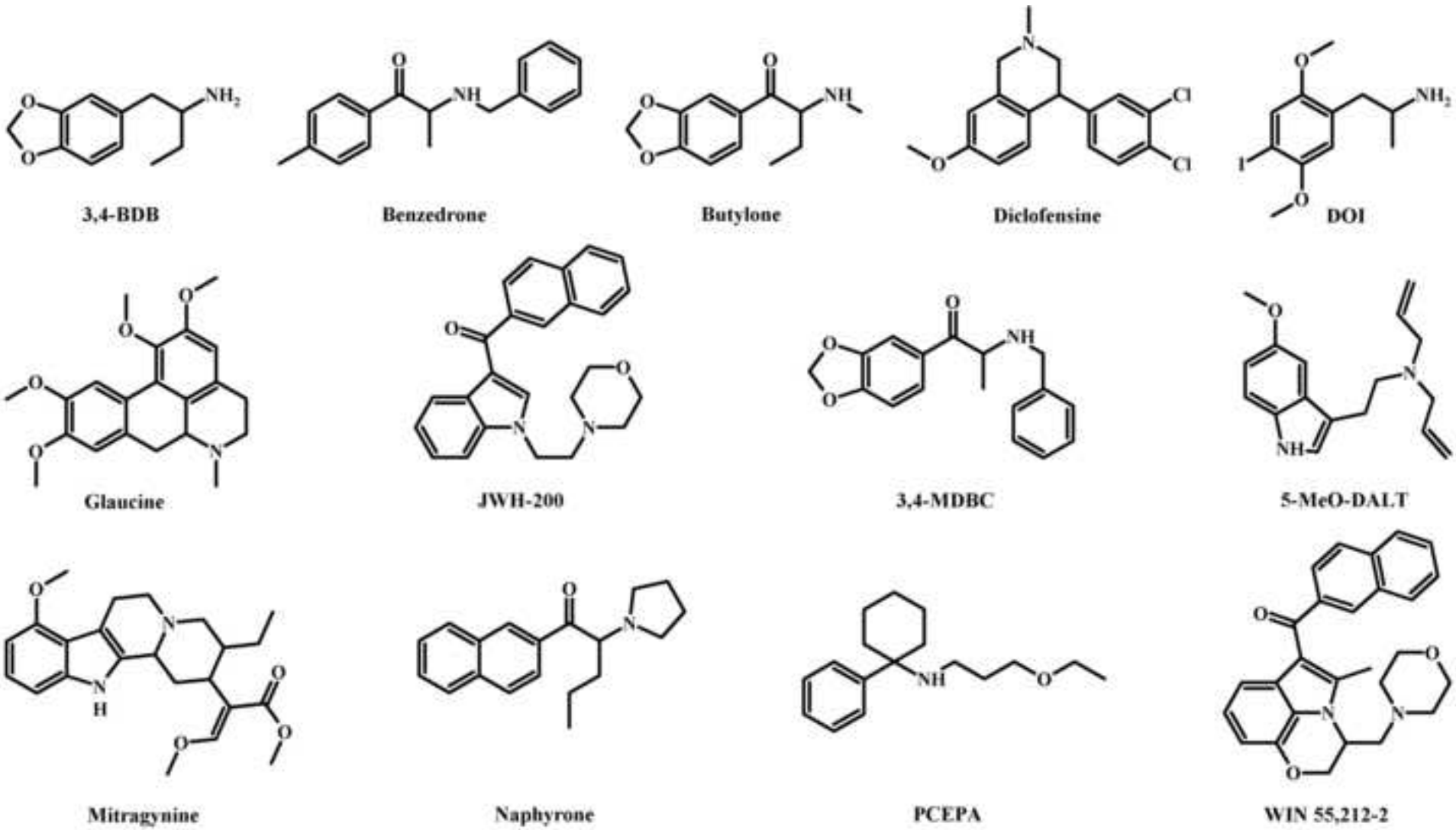

Figure 2

Click here to download Figure Fig_2.tif

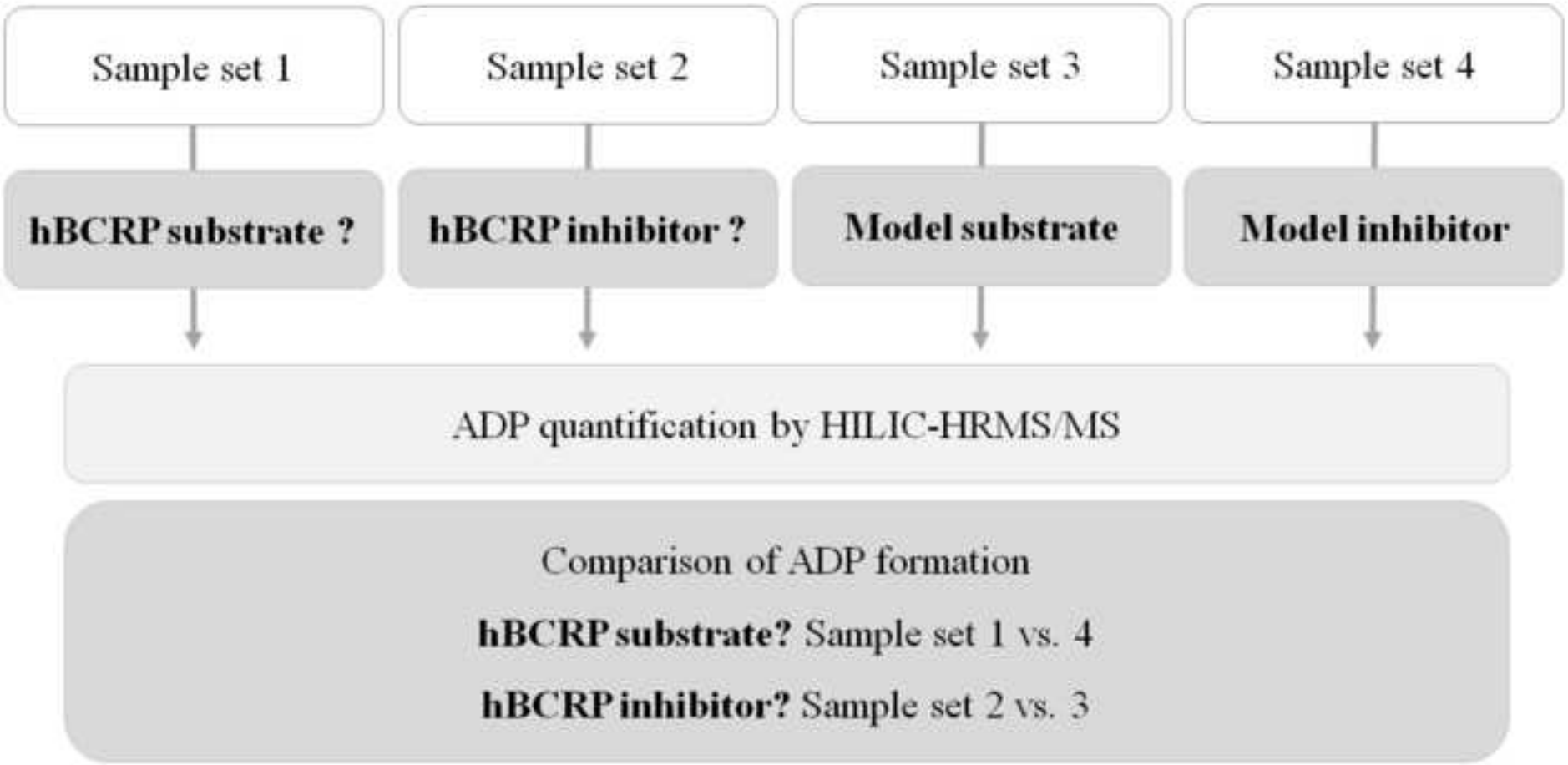

Figure 3

Click here to download Figure Fig_3.tif

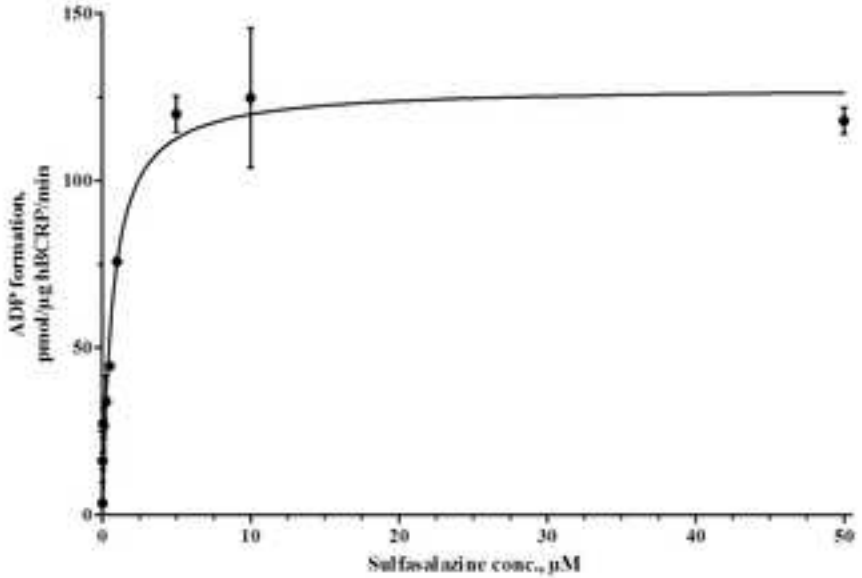

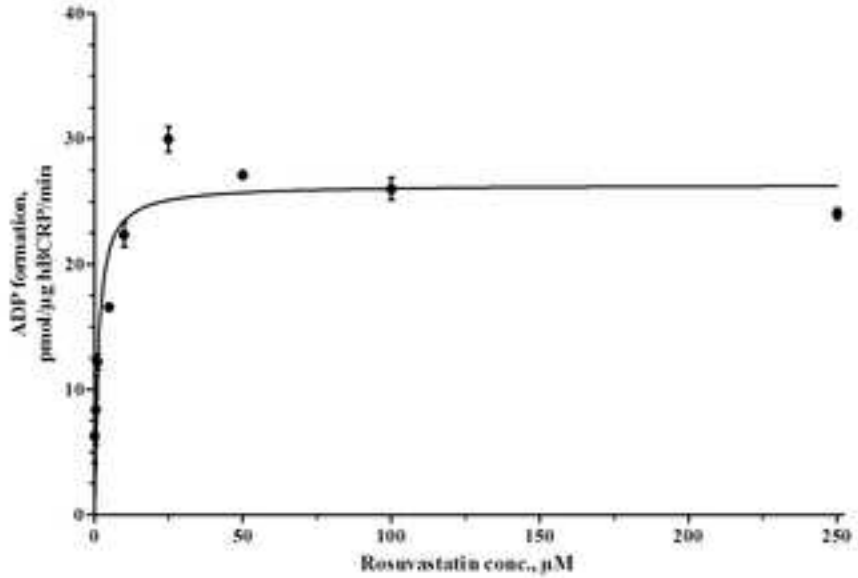

Figure 4

Click here to download Figure Fig_4.tif